

# Three-dimensional Crack Growth Simulations: Computational Aspects and Analysis of Crack Tunneling to Quantify COD as a Function of Constraint

Michael A. Sutton<sup>1</sup>, Xiaomin Deng<sup>1</sup> and Jianzheng Zuo<sup>1</sup>

<sup>1</sup>Department of Mechanical Engineering, University of South Carolina, Columbia, SC 29208

## ABSTRACT

An important task in mixed-mode fracture analysis and prediction is the simulation of crack growth under mixed-mode conditions. To complete such a task, one must have (a) a computer code capable of handling both the kinematics of general crack growth and also the determination of the stress and deformation states during crack growth, and (b) a fracture criterion that can properly predict the instant and direction of crack growth. A current challenge is the simulation of mixed-mode crack growth under three-dimensional (3D) conditions, such as the growth of surface cracks, corner cracks, embedded cracks, and cracks with a curved crack surface and/or a curved crack front.

In this work, we will present a brief summary of recent work directed towards computational aspects of a simulation procedure and associated algorithms for simulating arbitrary 3D crack growth under general loading conditions that have been developed and successfully implemented by the authors in a custom, finite element based, crack growth analysis and simulation code CRACK3D. In particular, this paper will present strategies for automatic re-meshing of regions around growing crack fronts in a 3D body, and will discuss verification examples.

Then, an application of the simulation code to the detailed analysis of crack tunneling and slanting along measured crack surfaces will be presented [1]. Results of this investigation suggest that the critical COD [2,3] value has a clear dependence on the crack front stress constraint,  $A_m = \sigma_m / \sigma_e$ , where  $\sigma_m$  is the mean stress and  $\sigma_e$  is the von Mises effective stress. This dependence seems to be linear within the range of computed stress constraint values, with the critical COD decreasing with increasing constraint.

## 1 INTRODUCTION

Many approaches have been reported in the literature for three-dimensional mesh generation including the advancing front technique [4-12], with most methods utilizing tetrahedral elements during the generation process due to its suitability for modeling complex geometries.

For three-dimensional regions with crack-like flaws (e.g., surface, through-thickness, multiple) the automatic mesh generation process is difficult. Specifically, there are two features in flawed components that increase the complexity of the meshing and re-meshing procedures;

- geometric coincidence of crack surfaces where at least two nodes on separate crack surfaces share a common location and
- local penetration of crack surfaces when the surfaces are not represented by coincident nodes.

In the former case, it is essential that the appropriate node be identified so that elements can be generated that do not cross the fracture surface. In the latter case, local crack surface penetration is often expected after discretization of curved crack surfaces, resulting in intersecting volume elements. Due to the complex topology for these cases, none of the mesh generation methods in the literature consider both issues.

- The importance of developing approaches for 3D re-meshing for flawed geometries is related to the need to develop appropriate fracture criteria for specific material systems. For example, recent experimental results [13, 14] clearly demonstrate that crack tunneling

(often accompanied by fracture surface slanting) is present during the early stages of crack growth, even in thin-sheet ductile materials. Even though slanting is observed in some cases, all of these experiments show that crack tunneling occurs under Mode I loading, regardless of whether the specimen is in a TL or LT orientation, suggesting that conditions at the centerline of the specimen result in the first increment of crack growth.

In this work, a brief discussion of techniques developed and implemented in the custom code, CRACK3D, to remesh along crack fronts is presented. Then, results from applying CRACK3D to model a thin, single-edge cracked specimen and quantify crack opening displacement (COD) as a function of stress constraint are discussed.

## 2 ADVANCED REMESHING APPROACHES FOR FLAWS

The Advancing Front Technique (AFT) is one of the most popular mesh generation methods [4-8]. According to the standard approach used in AFT, a valid element is defined such that

- any one of the sides (edges) of the new element does not intersect any one of the existing facets on the mesh generation front
- any one of facets of the new element does not intersect any one of existing sides (edges) on the mesh generation front.

For the case where two nodes on separate fracture surfaces are located at the same spatial position, or where local penetration of the separate fracture surfaces occurs locally, the standard AFT algorithm would result in an incorrect decision for the acceptance or rejection of a new element in the region near crack surfaces due to the local coincidence and/or penetration of crack surfaces. To overcome this difficulty, an enhanced AFT method was developed and used for mesh generation in structures with or without cracks. The method is described in detail in Reference 15. Specifically, algorithms have been written to properly mesh and remesh crack tip regions where

- *Two nodes on crack surfaces share the same common spatial location*
- *One node on a crack surface but without corresponding “image” node from the other crack surface*
- *Local penetration of crack surfaces*
  - *Determination of candidate nodes for development of valid finite elements in regions of penetration*
- *Modification of local mesh generation front during meshing process, resulting in the identification and removal of ill-shaped elements*

Without loss of generality, the four algorithms developed to address the issues noted above have been shown to be both robust and effective when used to re-mesh a wide range of flawed and unflawed specimen geometries.

### 2.1 Measurement of Mesh Quality

Various measures of mesh quality have been proposed in the literature to characterize the shape of tetrahedral element [16-18]. In this work we use the measure of tetrahedral mesh quality proposed in [18] which has a range from zero (least quality) to one (best quality). The following definition of mesh quality is used to measure the mesh quality.

$$\gamma(N) = \chi * V(N) * L^{1.5} \quad (1)$$

where  $V(N)$  is the volume of tetrahedral element  $N$ ,  $\chi$  is a normalized factor so that an equilateral tetrahedral element will have a maximum value of one. Specifically,  $\chi = 72\sqrt{3}$  is used in the work and  $L$  is the sum of square of the length of all six sides (edges) in element  $K$ . Figure 1 shows the mesh for a surface-cracked solid after employing the meshing algorithms, where the number of elements is  $\sim 73,000$ . Based on the quality measure given above, the minimum element quality  $\gamma=0.27$ , the maximum element quality  $\gamma=1$  and the average quality of the entire mesh  $\gamma=0.82$ .

### 3 APPLICATION TO DETERMINE COD AS A FUNCTION OF CONSTRAINT

Figure 2 shows the single edge-cracked specimen geometry. The specimen is machined from rolled 2.3mm-thick sheets made of aluminum alloy 2024-T351 and pre-cracked in the LT orientation with an initial crack length to specimen width,  $a/w = 0.0833$  [1]. To assess the level of crack tunneling in the presence of crack surface slanting, the procedure described in [19] was used to obtain crack front profiles on the non-planar fracture surfaces. Figure 3 shows the projected shape of the crack front profiles. The non-planar fracture surface shape (see Fig. 4 for a finite element representation) was measured using the procedures outlined in [13].

To determine constraint along the crack fronts shown in Fig. 3, the finite element code CRACK3D is used to analyze the stable tearing crack growth experiments. Initial mesh generation and post-analysis determination of stress and deformation states at various positions ahead of the current crack front are determined using the commercial code ANSYS. In this study, the nodal release option in CRACK3D is used to advance each crack front along the prescribed 3D fracture surface from the current crack front to the next one. Crack extension is accomplished through the release of nodal pairs (the two nodes in a pair are initially tied together by rigid springs) along the crack path when a certain condition is met. Crack extension along the crack front in the FE model is enforced when the load level reaches the value at which crack extension was observed (and the crack front is marked by fatigue) in the experiment.

#### 3.1 COD and Constraint During Stable Tearing

The variation in total COD at a distance of 0.5 mm behind the crack front (along a line normal to the crack front) for crack fronts 3 through 6 is shown in Figure 5. The through-thickness position in Fig. 5 refers to the  $z$  coordinate value along the crack front. Results for crack fronts in the early stage of crack growth are not shown because these crack fronts have growth only in the middle section and do not provide reliable critical values along parts of the crack front that are not at the impending moment of growth.

The variation in constraint,  $A_m = \sigma_m / \sigma_c$ , along crack fronts 3 through 6 is shown in Figure 6. The constraint value at each crack front point is computed based on an integrated average from the crack front to 0.3 mm ahead of the crack front, in the direction normal to the crack front and within the plane of the crack surface. It must be pointed out that, at and very near the specimen's front and back surfaces, a distance of 0.3mm ahead of a crack front may go outside the specimen domain. In this case, the constraint value for the next interior crack front point is used to approximate the constraint value for the current crack front point.

Figure 7 shows the relationship between critical COD and constraint for crack fronts 3 through 6.

### 4 DISCUSSION OF RESULTS

The computational strategies and algorithms developed have been shown to eliminate difficulties associated with automated (re-)meshing of 3D structures, with and without geometric discontinuities. Applications have shown that it is numerically stable, generating well-shaped elements in crack front regions and in far-field regions removed from the crack front.

Application of CRACK3D to the modeling of stable tearing in a single edge-cracked 2024-T351 aluminum specimen shows that there exists a nearly linear relationship between stress constraint and critical COD, with higher constraint values corresponding to lower levels of critical COD. The results are consistent with a recent void-growth study [20] which demonstrated a clear relationship between  $\sigma_m$  and  $\sigma_c$  during ductile failure. Based on their results, the authors suggested that there should be a relationship  $COD(A_m)$  at the onset of crack extension.

Thus, crack tunneling may be interpreted as the result of a lower critical COD near the mid-thickness of the crack front where higher constraint is present and a higher critical COD near the specimen's front and back surfaces, where lower constraint exists.

### 5 ACKNOWLEDGEMENTS

The authors gratefully acknowledge the technical assistance provide by Lt. Col. Scott Fawaz and Dr. James Harter, as well as the financial support from AFRL (Contract No. 00-3210-27-1). In addition, the technical support by Dr. Charles Harris and Dr. Robert Piascik, as well as the financial support from Dr. Julius Dasch at NASA HQ (Grant No. NCC5-174) is deeply appreciated.

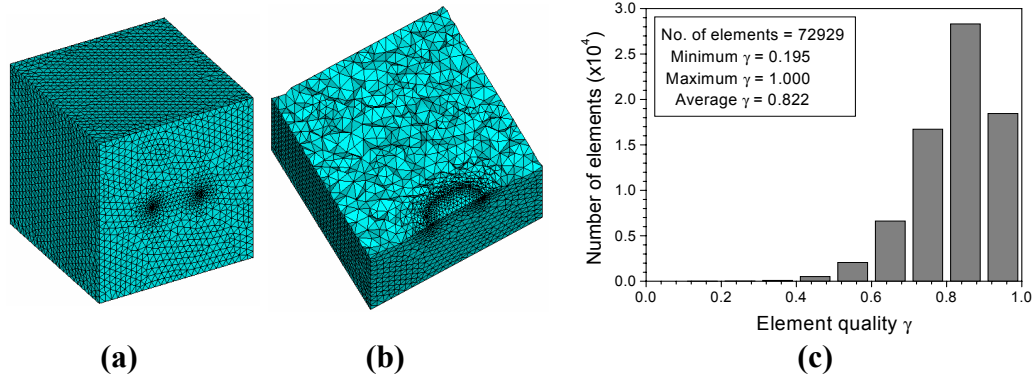


Figure 1: Automatically generated mesh of a cubic solid with a surface crack: (a) general view of the mesh; (b) mesh cross-section along crack surface; (c) mesh quality distribution.

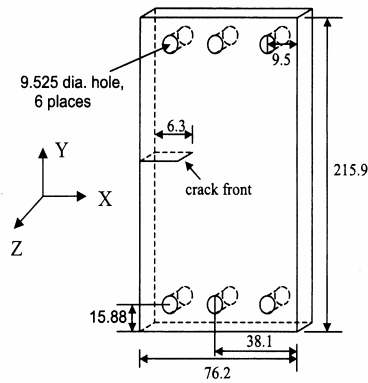


Figure 2: Schematic of a single-edge crack specimen

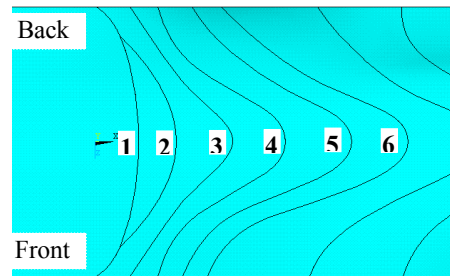


Figure 3: Crack front profiles

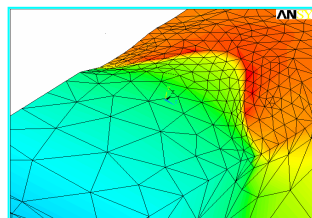


Figure 4: Finite element representation of 3D crack surface shape and crack front profiles for stable tearing analysis of single edge-cracked specimen under Mode I loading

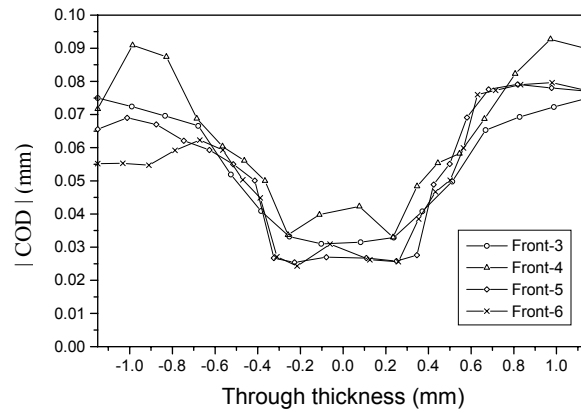


Figure 5: Variation of the magnitude in COD along crack fronts 3-6 at 0.5 mm behind the crack front.

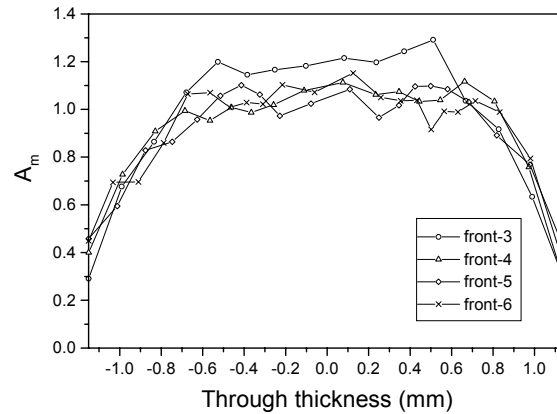


Figure 6: Variation of stress constraint  $A_m$  along crack fronts 3-6 averaged over 0.30mm ahead of current crack front

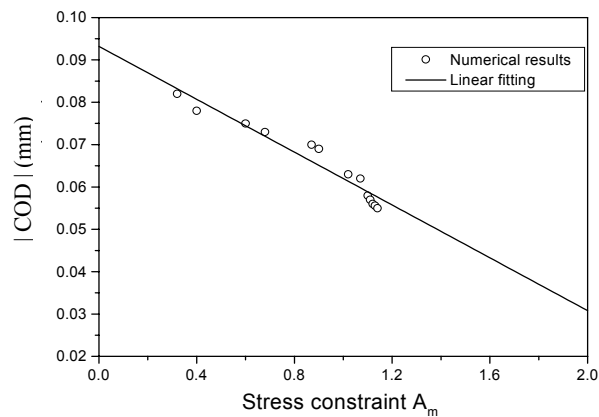


Figure 7: Critical COD as a function of stress constraint  $A_m$

## 6 REFERENCES

1. Boone, M. L., "Characterization of stable tearing in thin sheet of 2024-T3 aluminum alloy under tension-torsion loading conditions," Master Thesis, 1999, Department of Mechanical Engineering, University of South Carolina.
2. Ma, F., Deng, X., Sutton, M. A., and Newman, J. C., Jr., "A CTOD-based mixed-mode Fracture criterion," Mixed-Mode Crack Behavior, ASTM STP 1999, **1359**: 86-110.
3. Sutton, M. A., Deng, X., Ma, F., J. C. Newman, Jr., and M. James, "Development and application of a crack tip opening displacement-based mixed mode fracture criterion," International Journal of Solids and Structures 2000, **37**: 3591-3618.
4. Peraire J, Vahdati M, Morgan K, Zienkiewics OC. Adaptive remeshing for compressible flow computations. *Journal of Computational Physics* 1987; **72**:449-466.
5. Peraire J, Peiro J, Formaggia L, Morgan K, Zienkiewics OC. Finite element Euler Computations in three dimensions. *International Journal for Numerical methods in Engineering* 1988; **26**:2135-2159.
6. Peraire J, Peiro J, Morgan K. Adaptive remeshing for three-dimensional compressible flow computations. *Journal of Computational Physics* 1992; **103**:269-285.
7. Moller P, Hansbo P. On advancing front mesh generation in three dimensions. *International Journal for Numerical methods in Engineering* 1995; **38**:3551-3569.
8. Lohner R and Parikh P. Generation of three-dimensional unstructured grids by the advancing front method. *International Journal for Numerical methods in Fluids* 1988; **8**:1135-1149.
9. Lo SH. A new mesh generation scheme for arbitrary planar domains. *International Journal for Numerical methods in Engineering* 1985; **21**:1403-1426.
10. Zuo J, Lou ZW, Zhang HT. Automatic mesh generation algorithm and its application for arbitrary multi-connected regions. *Chinese Journal of Computational Structural Mechanics and Applications* 1995; **12**:80-85.
11. Zuo J, Lou ZW. Automatic mesh generation and adaptivity algorithm for finite element analysis. *Chinese Journal of Applied Mechanics* 1996; **13**:64-68.
12. Radovitzky R, Ortiz M. Tetrahedral mesh generation based on node insertion in crystal lattice arrangements and advancing-front-delaunay triangulation. *Computer Methods in Applied mechanics and Engineering* 2000; **187**:543-569.
13. Sutton, M. A., Helm, J. D. and Boone, M. L., Experimental study of crack growth in thin sheet 2024-T3 aluminum under tension-torsion loading. International Journal of Fracture, 2001, **109**: 285-301.
14. James, M.A. and Newman Jr. J.C., The effect of crack tunneling on crack growth: experiments and CTOA analysis. Engineering Fracture Mechanics, 2003, **70**: 457-468, 2003.
15. Zuo, J., Deng, X. and Sutton, M.A., Tetrahedral mesh generation in three-dimensional domains with cracks, International Journal for Numerical Methods in Engineering (in review).
16. Parthasarathy VN, Graichen CM, Hathaway AF. A comparison of tetrahedron quality measures. *Finite Elements Analysis Design* 1993; **15**:255-261.
17. Liu A, Joe B. Relationship between tetrahedron shape measures. *BIT* 1994; **34**:268-287.
18. Lo SH. Volume discretization into tetrahedral — II. 3D triangulation by advancing front approach. *Computers & Structures* 1991; **39**:501-511.
19. Dawicke, D.S. and Sutton, M.A., CTOA and crack tunneling measurements in thin sheet 2024-T3 aluminum alloy, Experimental Mechanics, 1994, **34**: 357-368, 1994.
20. Zuo, J., Sutton, M.A. and Deng, X., Basic studies of ductile failure processes and implications for fracture prediction, Fatigue & Fracture of Engineering Materials & Structures, 2004, **27**: 231-243.